INL/CON-21-65136-Revision-0

Pellet Cladding Mechanical Interaction as a Potential Failure Mechanism During a Control Rod Drop Accident in a Boiling Water Reactor

May 2022

Kyle A Gamble, Aysenur Toptan, Pierre-Clement A Simon, Aaron Graham, Mehdi Asgari, Baris Sarikaya, James Tusar, Moussa Mahgerefteh

Changing the World's Energy Future

INL is a U.S. Department of Energy National Laboratory operated by Battelle Energy Alliance, LLC

INL/CON-21-65136-Revision-0

Pellet Cladding Mechanical Interaction as a Potential Failure Mechanism During a Control Rod Drop Accident in a Boiling Water Reactor

Kyle A Gamble, Aysenur Toptan, Pierre-Clement A Simon, Aaron Graham, Mehdi Asgari, Baris Sarikaya, James Tusar, Moussa Mahgerefteh

May 2022

Idaho National Laboratory
Idaho Falls, Idaho 83415

http://www.inl.gov

Prepared for the
U.S. Department of Energy
Under DOE Idaho Operations Office
Contract DE-AC07-05ID14517

Pellet Cladding Mechanical Interaction as a Potential Failure Mechanism During a Control Rod Drop Accident in a Boiling Water Reactor

Kyle A. Gamble[1], Aysenur Toptan[1], Pierre-Clément A. Simon[1], Aaron Graham[2], Mehdi Asgari[2], Baris Sarikaya[3], James Tusar[3], and Moussa Mahgerefteh[3]

[1]Idaho National Laboratory
Computational Mechanics and Materials, P.O. Box 1625, Idaho Falls, ID 83415

[2]Oak Ridge National Laboratory
Nuclear Energy & Fuel Cycle Division,
Oak Ridge National Laboratory, One Bethel Valley Rd., Oak Ridge, TN 37831-6172

[3]Constellation
Nuclear Fuels, 200 Exelon Way, Kennett Square, PA 19348

kyle.gamble@inl.gov, aysenur.toptan@inl.gov, pierreclement.simon@inl.gov, grahamam@ornl.gov, asgarim@ornl.gov, baris.sarikaya@constellation.com, james.tusar@constellation.com, moussa.mahgerefteh@constellation.com

doi.org/10.13182/PHYSOR22-37711

ABSTRACT

Boiling water reactors (BWRs) represent approximately one-third of the operating fleet in the United States, contributing significantly towards the global effort in reducing carbon emissions. Even though most of the operating fleet has been in operation for quite some time, continued advancements in new nuclear fuel (such as accident tolerant fuel) or operating regimes (such as power uprates and higher burnup operation) necessitates similar advancements in modeling and simulation capabilities.

Bison, a component of the Virtual Environment for Reactor Applications (VERA), is a high-fidelity fuel performance code able to explore the fuel performance of a wide variety of fuel types in one-, two-, and three-dimensions. Until recently, the code had not been used for analyses of BWRs. Modeling capabilities have been added for Gd-bearing UO_2 and pure zirconium liners. New models have been added based upon the U.S. Nuclear Regulatory Commission (NRC) guidelines for hydrogen pickup in Zircaloy-2 claddings and pellet-clad mechanical interaction (PCMI) failure during a reactivity insertion accident (RIA), known as a rod drop accident (CRDA) in BWRs.

Implementing and/or improving Bison modeling capabilities extended its analytical reach to areas beyond its original intended purpose. This paper demonstrates one of these capabilities as a proof of concept. Recently developed models enable Bison to provide an alternate approach for cladding integrity determination in CRDA evaluations, which currently use bounding conservative estimates. As part of this demonstration, NRC guidance on hydrogen-pickup and PCMI failure models were utilized in this research. Even though more research is needed in establishing right inputs and process in this area, this paper demonstrates Bison's ability to determine cladding integrity in a CRDA evaluation. This first of a kind demonstration is a proof of concept in this area, which could potentially be extended to a number of other areas where a more accurate cladding integrity determination would be needed.

KEYWORDS: Bison, VERA, CRDA, BWR, PCMI

1. INTRODUCTION

Previous research resulted in the implementation of various thermo-mechanical properties [1] for boiling water reactor (BWR) materials (Gd-bearing UO_2 and liners) into the Bison fuel performance code [2] and investigated the sensitivity of the various models during normal operation on fuel performance metrics of interest (e.g., temperatures, stresses, and fission gas release) [3]. The specification and the detailed information for the assembly analyzed there were obtained from reference [4] documentation. In this study, we extend our analysis to assess the potential of pellet-clad mechanical interaction (PCMI) failure under various rod drop accidents (CRDAs) for three select rods from the same assembly (UO_2 fueled full length rod, a UO_2 partial length rod, and a full length rod containing UO_2 with Gd_2O_3). Both cold zero power (CZP) and hot zero power (HZP) conditions are considered for both fresh and burned fuel rods. The model describing hydrogen pick up, hydrogen precipitation and dissolution, and the failure limit suggested by the U.S. Nuclear Regulatory Commission (NRC) in Ref. [5] are first described in Section 2. The details, results, and analysis of the study of cladding failure during CRDAs are provided in Section 3. The conclusions drawn from this study are then summarized in Section 4.

2. HYDROGEN BEHAVIOR MATERIAL MODELS AND FAILURE LIMITS

The material behavior models addressed in this section cover a hydrogen pickup model for zirconium alloys cladding according to the NRC's Regulatory Guide (RG) 1.236 (Section 2.1), a hydrogen diffusion, precipitation, and dissolution model in cladding material (Section 2.2), and failure criterion specific to reactivity insertion accident (RIA) events (Section 2.3).

2.1. Hydrogen Pickup

For Zircaloy-2, primarily used as cladding material in a BWR, the NRC's RG 1.236 describes the hydrogen concentration a function of local axial burnup, Bu (GWd/MTU) of the fuel adjacent to the cladding [5]. This Zircaloy-2 burnup-dependent hydrogen content is given by

$$C_H = 1.40 \times \begin{cases} 47.8 \left[\exp\left(-\frac{1.3}{[1+Bu]}\right) + 0.316Bu\right], & Bu < 50 \text{ GWd/MTU} \\ 28.9 + \exp\left(0.117\left[Bu - 20\right]\right), & Bu > 50 \text{ GWd/MTU} \end{cases} \tag{1}$$

and shown in Fig. 1a. It is important to observe in Fig. 1a that the Eq. 1 states that the amount of hydrogen is equal to C_H=18.238 wt.ppm at zero burnup, rather than zero wt.ppm. Therefore, 18.238 wt.ppm of hydrogen should be initially added to the cladding for the simulation to match the equation provided in Ref. [5].

The flux is derived as $J = \frac{V}{S}\frac{dC_H}{dt}$ where the local axial burnup is time dependent and V/S depends on geometry, $V/S = L$ for plate specimens, and $V/S = L\left(1.0 - L/2r_{out}\right)$ for cylindrical specimens. No conversion factor is necessary for this correlation as the correlation returns a value in wt.ppm. Thus, for the Zircaloy-2 hydrogen model, the flux boundary condition is expressed as

$$J = \frac{V}{S}\frac{dBu}{dt} \times \begin{cases} \left[\frac{86.996}{(1+Bu)^2}\exp\left(\frac{-1.3}{1+Bu}\right) + 0.4424\right], & \text{for } Bu \leq 50 \text{ GWd/MTU} \\ 0.1638\exp\left(0.117\left[Bu - 20.0\right]\right), & \text{for } Bu > 50 \text{ GWd/MTU.} \end{cases} \tag{2}$$

2.2. Hydrogen Diffusion, Precipitation, and Dissolution Model

Once the hydrogen has been picked up by the cladding, it redistributes in the cladding following temperature, concentration, and stress gradients [6]. When the local concentration reaches the solubility limit, the hydrogen precipitates into zirconium hydrides. The description of hydrogen behavior during diffusion, precipitation, and dissolution has been recently improved in Refs. [7–9]. The latest version of the Hydride

Nucleation Growth Dissolution (HNGD) model has been implemented in Bison and applied to an out-of-pile configuration in the case of a Zircaloy-2 cladding with a Zr liner in Ref. [9]. In this study, the hydrogen behavior is simulated using the the model presented in Ref. [9] with the parameters listed in Table I.

Table I: Inner liner solubility and supersolubility parameters measured by [10,11].

Cladding	TSS_{D0} (wt.ppm)	Q_D (J/mol)	TSS_{P0} (wt.ppm)	Q_P (J/mol)
Zircaloy-2	14.3×10^3	36.7×10^3	32.7×10^3	25.0×10^3
Zirconium	14.1×10^3	38.1×10^3	33.9×10^3	27.3×10^3

2.3. Failure Criterion

Bison computes the failure of Zircaloy-2 cladding due to PCMI under RIA conditions. The failure criteria are functions of peak radial average fuel enthalpy rise and cladding excess hydrogen where excess hydrogen corresponds to the amount of hydrogen in hydrides [5]. Figure 1b shows the change in the peak radial average fuel enthalpy rise with respect to the excess cladding hydrogen for lined and unlined Zircaloy-2 claddings. The critical value for increase in peak radial average enthalpy, ΔH_{fail} is expressed in Ref. [5] as:

$$\Delta H_{\text{fail}} = \begin{cases} \min\left(150, 4.5\times10^5 C_{\text{prec}}^{-n} + 33\right), & T \leq 533.15 \text{ K} \\ \min\left(150, 5.5\times10^5 C_{\text{prec}}^{-n} + 50\right), & T > 533.15 \text{ K} \end{cases} \tag{3}$$

with $n = 1.9$ for the lined cladding and $n = 2.0$ for the unlined cladding. Here, ΔH_{fail} (cal/g) is the threshold increase in peak radial average enthalpy allowed before failure, C_{prec} (wt.ppm) is the amount of hydrogen in hydride form, and T (K) is the cladding temperature at the start of the transient.

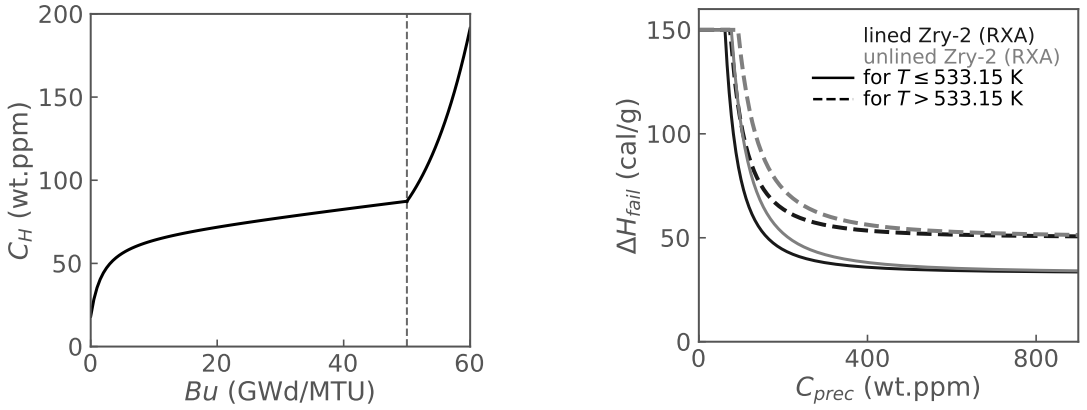

(a) **(b)**

Figure 1: (a) The hydrogen uptake model for Zircaloy-2 cladding as a function of burnup. (b) PCMI cladding failure threshold for lined and unlined Zircaloy-2 according to NRC RG 1.236 [5]. Note that the hydrogen uptake model assumes a non-zero value of hydride content of 18.238 ppm at 0 burnup.

3. RESULTS AND ANALYSIS

3.1. Problem Settings

Pulse shape A Gaussian pulse shape was employed in the RIA analyses RIA analyses in this study, which is expressed as Eq. 4 in terms of the full width at half maximum (FWHM), the maximum power, $P_{\max}$, and the maximum time, $t_{\max}$ in which the pulse exhibits. The FWHM for a Gaussian is found by finding the half-maximum points. The following relation is obtained between FWHM and $\sigma = 2.3548/\text{FWHM}$. This relation is plugged into Eq. 4 to have an expression in terms of pulse shape characteristics.

$$\frac{P(t)}{P_{\max}} = \frac{2.3548}{\text{FWHM}\sqrt{2\pi}} \exp\left(-\frac{[t - t_{\max}]^2}{2\left(\frac{\text{FWHM}}{2.3548}\right)^2}\right) \tag{4}$$

Fuel rod characteristics The layered one-dimensional (1-D) internal meshing capability is used for calculation efficiency, which meshes represent the fuel rod as a stack of 1-D radial slices assuming axisymmetric about the rod central axis. Each layer uses a generalized plane strain formulation to account for out-of-plane effects and to calculate global rod quantities such as fission gas release and rod internal pressure. Each layer does not need to have the same associated thickness. Since the axial positions used in the Virtual Environment for Reactor Applications (VERA) calculation, which produced the axial peaking factors used in this study, were not equidistant to one another, non-uniform slice heights were used. A single cladding (and liner) only layer is used for the plenum region.

The assembly analyzed in this work is based on one of the progression problems in Ref. [4]. Many different types of fuel pins are present, including full length and partial length rods. All rods contain natural uranium pellets above and below the enriched or gadolinia doped pellets. The length of the different fuel types can vary among the different rods, and the plenum heights are different between full length rods with and without gadolinia. The top and bottom plugs are also not modeled in this analysis. Additional axial pressures must be applied to the fuel and cladding materials to account for out-of-plane stress loading present due to the plenum and coolant pressures (P_{plenum} and P_{coolant}). For the fuel, the axial out-of-plane pressure is simply the plenum pressure. For the cladding and liner, the axial pressure P_{axial} is

$$P_{\text{axial}} = \frac{P_{\text{coolant}} D_{\text{co}}^2 - P_{\text{plenum}} D_{\text{ci}}^2}{D_{\text{co}}^2 - D_{\text{ci}}^2} \tag{5}$$

where D_{co} and D_{ci} are the cladding outer and inner diameter, respectively.

The nominal dimensions of the rods are a fuel radius of 4.8 mm, initial fuel-to-clad gap size of 90 μm, and cladding thickness of 0.68 mm (of which it is assumed 10% corresponds to the liner). The full length rods are $\sim$4.051 m long, whereas the partial length rods are $\sim$2.525 m long. The individual lengths of the various fuel types in the variety of rods within the assembly can be found in Ref. [4]. The plenum length is also different depending upon the type of fuel rod analyzed.

Thermo-mechanical models The physics included in the analysis depends upon the material. UO_2 and Gd_2O_3-bearing UO_2 models are included to account for elasticity, thermal conductivity, specific heat, cracking, thermal and irradiation creep, radial relocation, thermal expansion, densification, solid swelling, gaseous swelling, and fission gas release. The effect of Gd_2O_3 is captured through thermal conductivity and the radial power factor [12]. In the cladding and the liner, models are included for elasticity, thermal conductivity, specific heat, thermal creep, and thermal expansion. The model for the cladding also includes irradiation creep and irradiation growth. Details on each of the models can be found in the Bison online

documentation pages * and our previous work [1].

Boundary conditions Bison does not have an option for a two-phase flow thermal-hydraulic boundary condition internally. Ideally the coolant behavior would come from a subchannel code such at COBRA-TF (CTF) [13]. In this study, a simplistic Dirichlet type boundary condition is applied that fixes the temperature on the cladding surface. The temperature is linearly varied from a temperature of 551.15 K at the inlet to 560.15 K at the outlet as per Ref. [14]. Time-step evolution adapted based upon convergence difficulty as well as material behavior, in particular, creep of the fuel. An additional criterion is set that will terminate the simulation of any particular pin early if the rod internal pressure is calculated to be equal to or greater than the external coolant pressure of 7.17 MPa. See Ref. [3] for more details about power profiles.

3.2. Analysis of Control Rod Drop Accident on Fresh Fuel

A parametric study is performed here, where pulse characteristics are varied for the fresh fuel. According to Table II, the pulse width changes between 45 and 140 ms for HZP conditions and 45 and 75 ms for CZP conditions. Two cases, referred to as Case 1 and Case 2, were analyzed with a maximum powers, $P_{\max}$, of 400 and 700 MJ, respectively. The transient pulse begins at 1.0 seconds. To capture the details of the pulse in the vicinity of the peak, time-steps are explicitly reduced significantly, in addition to the adaptive time discretization scheme available in Bison. A flat axial power profile is assumed in these analyses. For CZP the cladding outside temperature was set to 295 K with atmospheric pressure, while for the HZP scenario the cladding outside temperature was set to 555 K at coolant pressure (7.17 MPa).

Table II: CRDA conditions for BWR from Ref. [15].

Parameter	CZP	HZP
Pulse width (ms)	45–75	45–140
Maximum fuel enthalpy (J/g)	140–460	160–400
Maximum enthalpy increase (J/g)	130–450	90–320
Rod worth (10^{-5})	700–1300	600–1300

The CRDA simulation results from our parametric study are provided here at CZP and HZP prior to the initiation of the transient for the selected fuel pins (1,1), (2,2), and (3,3) from the GE Assembly [4]: a full-length UO_2 rod, a partial-length UO_2 rod, and a full-length gadolinia doped UO_2 rod, respectively. Figure 2 shows the simulation results for radially averaged fuel enthalpy in each pin. Additionally, the shaded areas in the radial average enthalpy plot represent maximum fuel enthalpy ranges as tabulated in Table II for both CZP (140–460 J/g) and HZP (160–400 J/g). Other quantities of interest, from these simulations, are hydrogen content dissolved, hydrogen content in hydride, plenum temperature, plenum pressure, maximum clad hoop stress, maximum clad radial displacement, maximum fuel centerline temperature, and maximum fuel surface temperature. See Ref. [16] for the additional simulation results. From the simulations, the radially averaged fuel enthalpy lies in this region for the Case 1 and exceeds this region for the Case 2.

3.3. Analysis of Control Rod Drop Accident on Burned Fuel

The proposed PCMI failure criterion (see Figure 1b) is highly dependent on hydride content (called excess hydrogen in Ref. [5]) within the cladding. Therefore, the parametric study completed on fresh fuel is repeated here on burned fuel from the same assembly. The rods analyzed are the same pins from the fresh

*Bison: A Finite Element-Based Nuclear Fuel Performance Code, see https://mooseframework.inl.gov/bison/

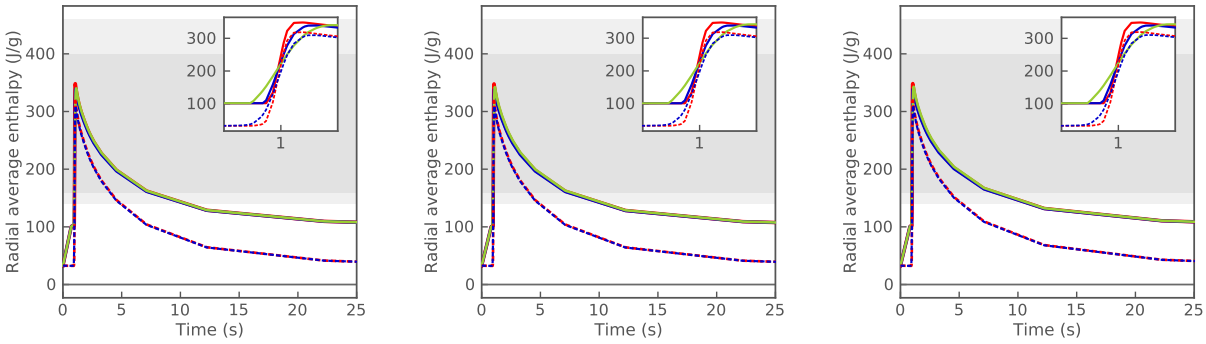

(a) Case 1: P_{max}=400 MJ

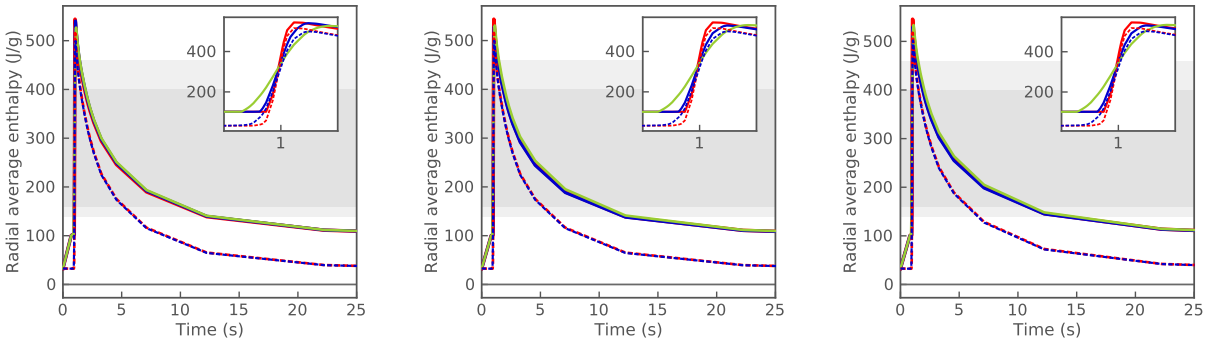

(b) Case 2: P_{max}=700 MJ

Figure 2: Simulation results for the fresh fuel pins at CZP (dashed lines) and HZP (solid lines): left plots for pin (1,1), center plots for pin (2,2), and right plots for pin (3,3). FWHM of 45, 75, and 135 ms are indicated in red, blue, and green, respectively.

fuel study; however, they have been subjected to the average linear heat rate and axial and radial profiles specific to each pin (see Ref. [3]). An additional termination criterion is added to the cases to stop the simulation when the radial average burnup in an particular layer exceeds the current regulatory limit of 62 MWd/kgU. This is done because the hydrogen pickup boundary condition (see Figure 1a) is only applicable to "approved commercial alloys up to their respective limits on fuel rod burnup, corrosion, and residence time" [5]. Even though the limits apply to rod average burnup for which these rods remain under, there is a significant axial profile in these rods that have local radial average burnups exceeding 75 MWd/tU if run for the full irradiation time. Using the hydrogen pickup model defined in Eq. 1 at these higher burnups quickly leads to excessive hydrogen content.

Instead of appending the RIA pulses at the end of the base irradiation, the hydride and hydrogen content at the end of the base irradiation from the peak axial layer is applied as initial conditions in the burned CRDA studies. The initial conditions for hydrogen and hydride content are provided in Table III. While this approach negates the effects of small gap sizes on the stress induced in the cladding during the transient, it is not necessary to account for these effects since the failure criterion utilized in this work only accounts for hydride content as a function of peak radial average enthalpy increase.

Figures 3 presents the results from the CRDA study on the burned pins for both CZP and HZP. Although part of the hydride phase is expected to dissolve when the temperatures increases, the duration of the transient is too short such that the hydride content remains very close to the initial value prescribed from

Table III: Hydride and hydrogen in solid solution contents for the fresh fuel simulations in the parametric study.

	Pin (1,1)	Pin (2,2)	Pin (3,3)
Hydride content (wt. ppm)	174.82	169.81	183.60
Hydrogen content (wt. ppm)	69.948	69.594	66.082

the base irradiation calculations. Given the values in Table III and comparing with the failure criterion for lined Zircaloy-2 in Figure 1b, these rods are expected to survive a peak radial average enthalpy increase close to 60 cal/g. By inspecting the radial average enthalpy injected in Figure 3, it is observed that this threshold is exceeded in all cases, even when limiting the maximum burnup to 62 MWd/kgU. Note that the cladding failure is indicated by a marker 'x.' This is a bit surprising given that some of the analyzed pulses are not that severe and are within the range found in the literature (see Table II). Further work is necessary to develop a new failure threshold that is a function of the radial concentration profile and orientation of the hydrides within the cladding and the impact on cladding embrittlement on a stress-based cladding failure criterion, as was initiated in Ref. [17].

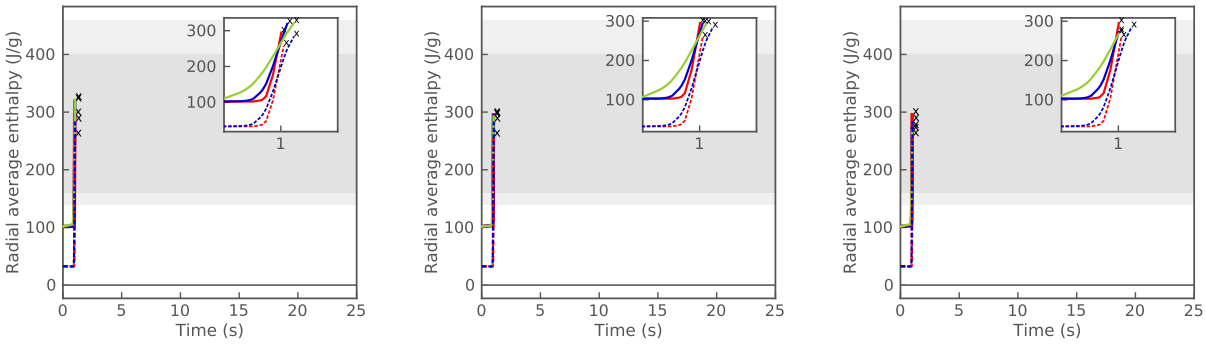

(a) Case 1: P_{max}=400 MJ

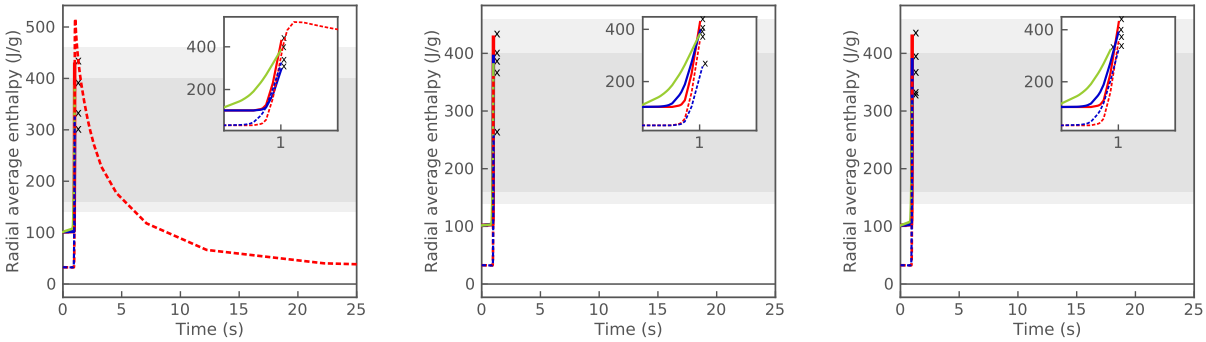

(b) Case 2: P_{max}=700 MJ

Figure 3: Simulation results for the burned fuel pins at CZP (dashed lines) and HZP (solid lines): left plots for pin (1,1), center plots for pin (2,2), and right plots for pin (3,3) FWHM of 45, 75, and 135 ms are indicated in red, blue, and green, respectively.

4. CONCLUSIONS AND FUTURE WORK

The Bison fuel performance code has been under development for about a decade. Over the years, developments have focused primarily on pressurized water reactor (PWR) materials including potential accident tolerant fuel (ATF) concepts as well as advanced reactor fuels such as metallic and tri-structural isotropic (TRISO) fuel particles. Bison's modeling capability was extended to support BWR fuel modeling analysis through an industry funding opportunity announcement entitled "Modeling & Analysis of Exelon BWRs with VERA for Eigenvalue and Thermal Limits" [1,3,16].

This paper demonstrates a high fidelity approach that can be taken to analyze CRDAs in BWRs. It has also been highlighted that the new NRC suggested hydrogen pickup and PCMI failure models include conservatism and do not account for important physics associated with hydrides regarding PCMI. In particular, the failure criterion is based only on the hydride content in the cladding, whereas other, more important aspects could be included to predict failure. For example, hydride orientation and alignment across the thickness of the cladding has been shown to better correlate with failure behavior than hydride content [17]. Moreover, stress inside the cladding would also have an important role in the failure mechanism. Currently, the failure criterion predicts a failure for every RIA pulse subjected to the burned fuel rods. Refining the current criterion may alleviate some of these constraints, enable a more accurate evaluation capability, and potentially reduces the need for utility and/or vendor specific model development, review, and approval.

The methods used to develop the base irradiation histories from the Oak Ridge National Laboratory (ORNL) supplied assembly used VERA's steady-state and depletion calculation capabilities. In addition to these calculations, VERA can also perform transient calculations. This includes solving the time-dependent neutron transport calculation as well as the time-dependent thermal hydraulics. Transients are described in the input in terms of perturbations of state variables as a function of time. Such state variables include inlet flow conditions, outlet pressure, and control rod or control blade positions. For every time step in the transient calculation, 3D distributions of pin powers, fuel temperatures, coolant temperatures and densities, and other data of interest are produced. Reactivity is also calculated at each time step, which allows for calculation of dynamic reactivity coefficients such as dynamic rod worth.

For the BWR blade drop, the blade will be fully inserted for the steady-state calculation. After converging the steady-state calculation, the blade will be withdrawn completely from 0 steps to 48 steps at a rate of 6 steps per second for an 8-second transient calculation. All the data transient results mentioned previously will be available as a result of this calculation, but the primary one of interest for this work is the time-dependent power history of the fuel rods and thermal hydraulic conditions in close proximity to the control blade. These histories will allow for a closer analysis of the behavior of individual fuel rods that could be at risk of failure due to the blade movement. Even though more research is needed in establishing right inputs and process in this area, this paper demonstrates Bison's ability to determine cladding integrity in a CRDA evaluation. This first of a kind demonstration is a proof of concept in this area, which could potentially be extended to a number of other areas where a more accurate cladding integrity determination would be needed.

ACKNOWLEDGEMENTS

This research was supported by and performed in conjunction with the Consortium for Advanced Simulation of Light Water Reactors, an Energy Innovation Hub for Modeling and Simulation of Nuclear Reactors under U.S. Department of Energy Contract No. DE-AC07-05ID14517.

This research made use of the resources of the High Performance Computing Center at Idaho National Laboratory, which is supported by the Office of Nuclear Energy of the U.S. Department of Energy and the Nuclear Science User Facilities under Contract No. DE-AC07-05ID14517.

REFERENCES

[1] A. Toptan and K. Gamble. "FY20 BISON BWR fuel modeling capability: Material models." Tech. Rep. INL/EXT-20-59936, INL (2020).

[2] R. L. Williamson, J. D. Hales, S. R. Novascone, G. Pastore, K. A. Gamble, B. W. Spencer, W. Jiang, S. A. Pitts, A. Casagranda, D. Schwen, A. X. Zabriskie, A. Toptan, R. Gardner, C. Matthews, W. Liu, and H. Chen. "BISON: A Flexible Code for Advanced Simulation of the Performance of Multiple Nuclear Fuel Forms." *Nuclear Technology*, **207**(7), pp. 954–980 (2021).

[3] K. Gamble and A. Toptan. "FY21 BISON BWR fuel modeling capability: Sensitivity analysis during normal operation." Tech. Rep. INL/LTD-21-62647, INL (2021).

[4] C. Lawing, S. Palmtag, and M. Asgari. "BWR Progression Problems." Technical Report DRAFT, Oak Ridge National Laboratory (ORNL) (2020).

[5] P. Clifford. "Regulatory Guide RG 1.236: Pressurized-water reactor control rod ejection and boiling water reactor control drop accidents." Tech. rep., NRC (2020).

[6] A. T. Motta et al. "Hydrogen in zirconium alloys: A review." *J Nucl Mater*, **518**, pp. 440–460 (2019).

[7] E. Lacroix et al. "Zirconium Hydride Precipitation and Dissolution Kinetics in Zirconium Alloys." *Zirconium in the Nuclear Industry: 19th International Symposium*, pp. 67–91 (2021).

[8] F. Passelaigue et al. "Implementation and Validation of the Hydride Nucleation-Growth-Dissolution (HNGD) model in BISON." *J Nucl Mater*, **544**, p. 152683 (2021).

[9] F. Passelaigue, P.-C. A. Simon, and A. T. Motta. "Predicting the hydride rim by improving the solubility limits in the Hydride Nucleation-Growth-Dissolution (HNGD) model." *J Nucl Mater*, **558**, p. 153363 (2022).

[10] K. Une and S. Ishimoto. "Terminal solid solubility of hydrogen in unalloyed zirconium by differential scanning calorimetry." *J Nucl Sci Technol*, **41**, pp. 949–952 (2004).

[11] K. Une et al. "The terminal solid solubility of hydrogen in irradiated Zircaloy-2 and microscopic modeling of hydride behavior." *J Nucl Mater*, **1**, pp. 127–136 (2009).

[12] A. Toptan. *A Novel Approach to Improve Transient Fuel Performance Modeling in Multi-Physics Calculations*. Ph.D. thesis, NCSU (2019).

[13] R. K. Salko et al. "CTF 4.0 Theory Manual." Technical Report ORNL/TM-2019/1145, ORNL, Oak Ridge, TN (United States) (2019).

[14] A. Peakman et al. "Development of an equilibrium loading pattern and whole-core fuel performance assessment in the Advanced Boiling Water Reactor (ABWR) with UO_2 and U_3Si_2 fuels." *Prog Nucl*, **117**, p. 103053 (2019).

[15] NEA,OECD. "Nuclear Fuel Behaviour Under Reactivity-Initiated Accident (RIA) Conditions." State-of-the-art Report NEA/CSNI/R(2010)1, Nuclear Energy Agency (2010).

[16] K. A. Gamble, A. Toptan, and P.-C. A. Simon. "PCMI as a potential failure mechanism during a control rod drop accident in a BWR." Tech. Rep. INL/LTD-21-64690, INL (2021).

[17] P.-C. A. Simon et al. "Quantifying the effect of hydride microstructure on zirconium alloys embrittlement using image analysis." *J Nucl Mater*, **547**, p. 152817 (2021).